Published in final edited form as:
*Mol Cell Neurosci*. 2008 April ; 37(4): 781–793.

# Developmental regulation of GABAergic interneuron branching and synaptic development in the prefrontal cortex by soluble neural cell adhesion molecule

**Leann Hinkle Brennaman** and **Patricia F. Maness**
*Department of Biochemistry and Biophysics, and Silvio Conte Center for Schizophrenia Research, University of North Carolina School of Medicine, Chapel Hill, NC 27599*

## Abstract

Neural cell adhesion molecule, NCAM, is an important regulator of neuronal process outgrowth and synaptic plasticity. Transgenic mice that overexpress the soluble NCAM extracellular domain (NCAM-EC) have reduced GABAergic inhibitory and excitatory synapses, and altered behavioral phenotypes. Here, we examined the role of dysregulated NCAM shedding, modeled by overexpression of NCAM-EC, on development of GABAergic basket interneurons in the prefrontal cortex. NCAM-EC overexpression disrupted arborization of basket cells during the major period of axon/dendrite growth, resulting in decreased numbers of GAD65- and synaptophysin-positive perisomatic synapses. NCAM-EC transgenic protein interfered with interneuron branching during early postnatal stages when endogenous polysialylated (PSA) NCAM was converted to non-PSA isoforms. In cortical neuron cultures, soluble NCAM-EC acted as a dominant inhibitor of NCAM-dependent neurite branching and outgrowth. These findings suggested that excess soluble NCAM-EC reduces perisomatic innervation of cortical neurons by perturbing axonal/dendritic branching during cortical development.

### Keywords

NCAM; development; branching; interneuron; synapse

## INTRODUCTION

The neural cell adhesion molecule (NCAM) is a member of the immunoglobulin (Ig)-like superfamily of cell adhesion molecules. NCAM participates in homophilic and heterophilic interactions that induce signal transduction, axon/dendrite outgrowth, and synaptic plasticity (reviewed in (Hinkle and Maness 2006; Maness and Schachner 2007)). Through alternative splicing, three major NCAM isoforms of 120, 140 and 180 kDa are generated. NCAM140 and 180 are transmembrane isoforms that differ in the length of their cytoplasmic domain and have roles in axon/dendrite growth and synaptic plasticity, respectively. NCAM120 is linked to the membrane through a GPI anchor and is predominantly found in glia. NCAM-null mutant mice exhibit deficient hippocampal long-term potentiation (LTP, (Cremer 1998; Bukalo 2004; Stoenica 2006)), spatial learning (Cremer 1994; Bukalo 2004), and emotional memory (Stork

Corresponding author: Patricia F. Maness, Department of Biochemistry and Biophysics, CB#7260, 505 Mary Ellen Jones Building, University of North Carolina, Chapel Hill, NC 27599, srclab@med.unc.edu.

1997; Stork 1999), and they display synaptic abnormalities in the hippocampus (Cremer 1997) and at the neuromuscular junction (Polo-Parada 2001). NCAM can be modified by addition of α-2,8 neuraminic acid or polysialic acid (PSA, (Bruses and Rutishauser 2001)) to the fifth Ig domain by the polysialyltransferases PST and STX (Nakayama 1998; Angata and Fukuda 2003). Polysialylation of NCAM is most prominent in brain during development (Edelman and Chuong 1982), and serves to decrease NCAM homophilic binding affinity (Rutishauser 1988; Johnson 2005) to promote axonal/dendritic growth (Ulfig and Chan 2004; Brocco and Frasch 2006) and motility (Conchonaud 2007). However, the mechanisms that regulate NCAM during synaptic development are poorly understood.

Recently, NCAM was found to be subject to ectodomain shedding by proteolytic cleavage to release the entire NCAM extracellular region (NCAM-EC) as a soluble fragment (Vawter 2001; Diestel 2005; Hubschmann 2005; Hinkle 2006; Kalus 2006). This cleavage is mediated by proteases with characteristics of ADAM (a disintegrin and metalloprotease) family metalloproteases. Cleavage of NCAM decreases NCAM-dependent neurite growth and branching of primary cortical neurons (Hinkle 2006), but promotes neurite growth in hippocampal neuron cultures (Hubschmann 2005; Kalus 2006). An important question is whether the shed NCAM-EC cleavage fragment modulates these neuronal responses *in vivo*.

Abnormally high levels of the soluble cleavage fragment consisting of the entire extracellular region of NCAM (NCAM-EC) have been reported in affected brain regions of individuals with schizophrenia (van Kammen 1998; Vawter 2000; Vawter 2001), correlating with disease severity (Lyons 1988). Furthermore, PSA-NCAM is decreased in schizophrenic brain (Barbeau 1995), and single nucleotide polymorphisms (SNPs) in the STX gene are associated with schizophrenia in Japanese and Chinese Han subpopulations (Arai 2006; Tao 2007). Recently SNPs in the NCAM gene were found to be associated with neurocognitive impairments such as working memory in a large schizophrenia population (Sullivan 2007). Thus, abnormalities of NCAM expression or regulation could contribute to synaptic alterations that impair cortical function.

A transgenic mouse that overexpresses NCAM-EC from the onset of neuronal differentiation provides a model for investigating the effect of excessive NCAM shedding on synaptic development of cortical neurons. NCAM-EC mice display reduced numbers of GABAergic inhibitory synapses in the adult prefrontal cortex (PFC), and exhibit abnormal behaviors such as reduced prepulse inhibition of acoustic startle (PPI), impaired fear conditioning, and hyperactivity (Pillai-Nair 2005). One type of interneuron affected by NCAM-EC overexpression in the PFC is the GABAergic basket cell, which expresses parvalbumin and forms inhibitory perisomatic synapses at the soma of cortical pyramidal cells (Markram 2004; Lewis 2005). Perisomatic innervation by interneurons modulates output and synchronizes pyramidal neuron groups, which is thought to underlie working memory (Spencer 2003; Wang 2004; Lewis 2005; Huang 2007). The phenotype of NCAM-EC transgenic mice raises the possibility that soluble NCAM-EC may act as a dominant inhibitor of normal NCAM function; however it is not known whether NCAM-EC perturbs developmental NCAM functions, such as axonal/dendritic outgrowth and branching or only affects its mature synaptic role.

To investigate whether interneuron development in the PFC is affected by perturbing NCAM function through overexpression of the soluble NCAM-EC fragment, NCAM-EC mice were intercrossed to a fluorescent reporter strain in which a subclass of basket interneurons express enhanced green fluorescent protein (EGFP) from the GAD67 promoter (GAD67-EGFP) throughout the soma, axons and dendrites (Chattopadhyaya 2004). By analyzing development of perisomatic innervation by basket cell interneurons, we found that overexpression of NCAM-EC perturbed basket cell arborization during early postnatal development of the PFC,

consistent with a mechanism in which soluble NCAM-EC inhibits developmental NCAM interactions that regulate outgrowth and branching of interneuronal processes.

## MATERIALS AND METHODS

### Mice

Transgenic NCAM-EC (Pillai-Nair 2005) and GAD67-EGFP (Chattopadhyaya 2004) BAC transgenic mice (C57Bl/6 background) were intercrossed to obtain NCAM-EC/GAD67-EGFP mice and wild-type (WT)/GAD67-EGFP littermates. Embryonic day 0.5 (E0.5) was defined as the plug date and postnatal day 0 (P0) as the day of birth. All animals were used according to University of North Carolina at Chapel Hill Institutional Animal Care and Use Committee policies and in accordance with NIH guidelines.

### Immunochemicals

Antibodies used were actin monoclonal antibody (mAb) 1501, PSA mAb5324 (Chemicon, Temecula, CA), anti-PSA mAb (gift of Dr. Rita Gerardy-Schahn, Medical University of Hannover, Germany), NCAM polyclonal antibody (pAb) H300, synaptophysin pAb (Santa Cruz Biotechnology, Santa Cruz, CA), NCAM mAb OB11 (Sigma), GAD65 mAb (Developmental Studies Hybridoma Bank, University of Iowa, Iowa City, IA), neuronal specific class III β-tubulin TUJ1, HA mAb (Covance Research Products, Berkeley, CA), and normal human, rabbit and mouse IgG (Jackson ImmunoResearch, West Grove, PA). NCAM-Fc was generated as previously described (Meiri 1998).

### Neuronal culture and neurite outgrowth

Primary cortical neuron cultures were prepared from E16.5 mouse embryos. The cerebral cortex of the embryos was dissected and collected in complete Hank's Balanced Salt Solution (HBSS pH 7.3, 2.5 mM HEPES pH 7.4, 30 mM D-glucose, 1 mM $CaCl_2$, 1 mM $MgSO_4$, 4 mM $NaHCO_3$ (Polleux and Ghosh 2002)), and neurons dissociated with fire-polished Pasteur pipettes. Neurons were plated onto mouse L-fibroblast monolayers or L-fibroblasts stably expressing NCAM140 (Beggs 1994) in LabTekII chamber slides at a density of $1.5–2 \times 10^4$ cells per well for neurite outgrowth (Hinkle 2006). Neurons were cultured for 72 h in complete media (Dulbecco's modified Eagle's media with 5% fetal bovine serum (FBS, Hyclone) and penicillin/streptomycin (1X)). NCAM-Fc or normal human IgG (50 μg/ml) was added at the time of plating. Twenty-four to 36 h after plating, the media was replaced with complete media including NCAM-Fc or human IgG. At 72 h post plating, neurons were fixed in 4% paraformaldehyde and stained for neuronal class III β-tubulin (anti-TUJ1; 1:500) using AlexaFluor 488 conjugated secondary antibodies (1:400, Molecular Probes, Inc., Eugene, OR). Neurons were imaged on a Zeiss Axiovert 200 inverted microscope with an Axiocam MRc5 digital camera (Carl Zeiss Inc., Thornwood, NY). Neurites longer than 10 μm not in contact with any other neuron were measured by tracing the length of the single longest neurite (including branches) using ImageJ software. The percent of cells with branched neurites was calculated and analyzed for statistical significance using the one-tailed Student's t test ($p \leq 0.05$).

### Immunoblotting and immunoprecipitation

To generate brain homogenates, forebrains of WT mice (E18.5 to adult) were homogenized on ice in complete RIPA buffer containing phosphatase inhibitors (20 mM Tris-Cl pH 7.0, 0.15 M NaCl, 5 mM EDTA, 1 mM EGTA, 1% NP-40, 1% sodium deoxycholate, 0.1% SDS, protease inhibitor cocktail (Sigma), 1 mM phenylmethylsulfonylfluoride (PMSF), 0.1 mM sodium orthovanadate, 5 mM sodium fluoride). Lysates were clarified by centrifugation at 14000 × g, and protein concentration analyzed by bicinchronic acid (BCA) protein assay (Pierce). Total brain lysates (75 μg) were subjected to 7.5% SDS-PAGE and proteins

transferred to nitrocellulose membranes (Schleicher and Schuell Bioscience Inc., Keene, NH). Membranes were blocked in 5% milk in Tris buffered saline containing Tween-20 (TBS-T; 25 mM Tris pH 7.4, 140 mM NaCl, 2.7 mM KCl, 0.5% (v/v) Tween-20), and incubated for 1.5 h in primary antibodies: mouse anti-NCAM-ICD 1:1000 (clone OB11), rabbit anti-NCAM-ECD 1:500 (clone H300), mouse anti-PSA 1:200 (gift of Dr. Rita Gerardy-Schahn), mouse anti-PSA 1:750 (Chemicon), mouse anti-HA (hemagglutinin) 1:1000, or mouse anti-actin 1:5000. Membranes were rinsed in TBS-T and incubated for 1 h in horseradish peroxidase conjugated secondary antibodies (Jackson ImmunoResearch) at dilutions of 1:10000. Membranes were developed using enhanced chemiluminescence (Pierce) and exposed to film.

For immunoprecipitation, brain lysates (500 μg) from WT and NCAM-EC mice were incubated with anti-HA antibodies (10 μg/ml) or NCAM-ICD antibodies (clone OB11, 12.5 μg/ml) for 1 hour at 4°C in TNEN buffer (50 mM Tris pH 7.5, 150 mM NaCl, 1 mM EDTA, 0.5% NP-40) containing protease and phosphatase inhibitors, followed by protein G Sepharose (GE Healthcare) for 1 hour. Immune complexes were washed with TNEN buffer, and released by boiling in SDS-PAGE sample buffer.

### Morphometric analysis of basket cells

NCAM-EC/GAD67-EGFP and WT GAD67-EGFP littermate mice from P10 to adult (5 months) were anesthetized and perfused transcardially with 4% paraformaldehyde. Brains were postfixed in 4% paraformaldehyde for 1−2 days and embedded in agarose for Vibratome sectioning. Coronal sections (100 μm) were collected, and EGFP-labeled basket cells were analyzed in layers II/III of the anterior cingulate cortex. Individual neurons were imaged at equivalent rostrocaudal levels and reconstructed on an Olympus FV500 confocal laser scanning microscope using a 60X objective and 2.5X optical zoom at the University of North Carolina Microscopy Services Laboratory (Dr. Robert Bagnell, Director, Department of Pathology, University of North Carolina School of Medicine). Images were acquired using laser excitation 488 nm, 10% laser power and 105 μm aperture. Four to five mice per genotype per stage were analyzed. For each mouse, 30−50 individual basket cells were fully imaged and reconstructed. Optical sections ranged from 0.5−1.0 μm with 30−60 sections per z-stack. Neuronal density was scored by counting the number of EGFP-labeled basket cells from at least 5 randomly chosen fields from each animal used for morphometric analysis. A minimum of 100 cells per mouse were scored. Density was reported as number of cells/field.

Neurons were manually traced from confocal z-stack images (25−50 μm average total thickness) using Neurolucida® software (MBF Bioscience, Williston, VT) and analyzed using the NeuroExplorer module. Proximal neuronal arborization was analyzed from the soma to a distance 30 μm proximal to the soma, as neurites were not able to be accurately traced more distally. Axons and dendrites were grouped together and termed primary processes. Means were calculated for each genotype at a given developmental stage, and compared for statistical significance using the one-tailed Student's t test ($p<0.05$). For each neuron the following morphological features were measured:

1) Soma area. The cell soma area was outlined using Neurolucida, and somal area ($\mu m^2$) was automatically calculated.

2) Number of processes. Primary processes were defined as any axon or dendrite that exited the soma.

3) Total number of ends. Defined as the apparent number of process endings within 30 μm proximal to the soma as seen in the confocal z-stack image.

4) Branching index. Branching index was calculated as the total number of ends/total number of primary processes for each neuron evident in the z-stack images (Yelnik 1984; Aizenman 2003; Kondoh 2004).

5) Sholl analysis. Concentric circles were automatically drawn around the soma with 10 μm differences in diameter, and the total number of times the processes crossed each Sholl ring were automatically calculated. Analysis was performed at a distance of 20 μm from the soma. The mean number of crossings per process at a Sholl distance of 20 μm was calculated by dividing the total number of times the processes crossed this Sholl ring by the total number of processes for each neuron.

### Immunofluorescence and synapse analysis from GAD67-EGFP transgenic mice

NCAM-EC and WT mouse littermates (P10, P20, adult) were anesthetized and perfused transcardially with 4% paraformaldehyde. Brains were postfixed for 1−2 days in 4% paraformaldehyde, cryoprotected in 30% sucrose, then frozen and processed for cryostat sectioning (14 μm) (Demyanenko 1999). Sections were blocked in 5% milk/5% normal goat serum, and treated with 1% NP-40 for permeabilization. Sections incubated for 1 h in the following primary antibodies: 5 μg/ml mouse anti-GAD65 or 1:150 rabbit anti-synaptophysin. Sections incubated for 30 min in 1% serum containing Alexa488-conjugated (1:400; Molecular Probes, Eugene, OR) or TRITC-conjugated (1:200; Jackson ImmunoResearch, West Grove, PA) secondary antibodies, mounted in Vectashield (Vector Laboratories, Burlingame, CA), and imaged as described above, with the exception that individual optical slices were captured for each section. Images were analyzed using Scion Image. For EGFP-positive animals, 3−5 images from each z-stack (see above) were compressed to form a single image. At least 50 −100 neurons were analyzed per genotype per stage. Perisomatic signals (puncta rings) from at least 5 randomly chosen fields for each image were delineated and pixel density within the delineated area was computed and averaged as described previously (Huang 1999; Pillai-Nair 2005). The data were compared for statistically significant differences in mean values using the one-tailed Student's t-test ($p<0.05$).

## RESULTS

### Developmental regulation of NCAM expression, polysialylation, and ectodomain shedding

To analyze the developmental regulation of NCAM and its modification by polysialylation, the expression of NCAM isoforms and their polysialylation status were examined in mouse brain at developmental stages that corresponded to major periods of interneuronal differentiation (E18.5-P1), axon/dendrite outgrowth (P1-P10), synaptogenesis/remodeling (P20), and maturation (P40) (Lauder 1986; Vincent 1995; Flames 2004). Immunoblotting with an antibody specific for the polysialylic modification of NCAM (Fig. 1A) showed PSA-NCAM as a broad band of approximately 250 kDa that was present at highest levels in developing brain from E18.5 to P10, decreasing abruptly at P20 and almost undetectable at P40. Immunoblotting with antibodies directed against common determinants in the NCAM intracellular cytoplasmic domain (NCAM-ICD) of both NCAM140 and NCAM180 showed non-polysialylated NCAM isoforms appearing at P5-P10, and persisting from P20 to adult (P40) (Fig. 1A, second panel). Immunoblotting with antibodies directed against the NCAM extracellular domain (NCAM-ECD) revealed two NCAM ectodomain fragments of ~105 and 110 kDa that were present from E18.5 to P10, but undetectable at P20−40 (third panel, Fig. 1A). These fragments were not recognized by PSA antibodies (not shown). The ectodomain fragments were of similar sizes reported for the cleaved NCAM extracellular region, and may result from separate cleavage events (Bock 1987; Nybroe 1989; Krog 1992; Todaro 2004). The mobility of the NCAM-ECD protein fragments further suggested that they represented non-polysialylated fragments of the NCAM ectodomain. The corresponding NCAM-ICD

fragments resulting from cleavage of NCAM180 (~85 kDa) and NCAM140 (~30 kDa) were not apparent on immunoblots, and thus may be degraded intracellularly. Glial-associated NCAM120 was seen upon longer exposure times of the blots, and first appeared at P20 with higher levels in adult brain (Fig. 1A, bottom panel). This pattern was consistent with previous reports demonstrating that NCAM120 expression in the cortex begins at P14 and is highest in adult brain (Edelman and Chuong 1982).

NCAM-EC transgenic mice secrete the transgenic NCAM-EC protein (NCAM-EC$^{tg}$) at 50% of the total NCAM level in the brain (Pillai-Nair 2005). Previous studies have demonstrated that the strength of the NCAM-NCAM homophilic interaction ($K_d$ ~60 nM) is reduced approximately 5 fold by the addition of PSA (Johnson 2005; Kiselyov 2005). This facilitates axonal and dendritic growth and arborization (Ulfig and Chan 2004; Brocco and Frasch 2006) and prevents inappropriate synaptic connections (di Cristo 2007). As development progresses, PSA is downregulated to allow for synaptogenesis (di Cristo 2007; Gascon 2007). Thus, the inhibitory effects of NCAM-EC$^{tg}$ on inhibitory synapse number (Pillai-Nair 2005) could, in principle, occur if the transgenic fragment was polysialylated. To evaluate this possibility, the expression (left set of panels, Fig. 1B) and polysialylation (right set of panels, Fig. 1B) of NCAM-EC$^{tg}$ was analyzed in developing brain from early postnatal stages to adult. NCAM-EC$^{tg}$ protein contains a hemagglutinin (HA) epitope tag at its C-terminus, which can be detected by anti-HA antibodies. In NCAM-EC brain, NCAM-EC$^{tg}$ protein was present at roughly equivalent levels from P10 to adult as shown by immunoblotting of brain lysates using HA antibodies (Fig. 1B, top left panel). HA-tagged NCAM-EC protein was not detected in WT brain, as expected. To determine if NCAM-EC$^{tg}$ was polysialylated, brain lysates were immunoprecipitated with antibodies to the HA tag, followed by immunoblotting with antibodies to PSA (right set of panels, Fig. 1B). Although the HA antibodies successfully precipitated NCAM-EC$^{tg}$ at all stages (Fig. 1B, top right panel), NCAM-EC$^{tg}$ was not recognized by PSA antibodies at any stage, even with long exposure times (right middle panel). In contrast, full-length PSA-NCAM was present at equivalent levels in WT and NCAM-EC transgenic brain at P10, decreasing progressively from P20 to adult (Fig. 1B, left middle panel). Thus, the transgenic NCAM-EC protein did not contain detectable levels of PSA, and its pattern of expression did not affect levels of endogenous PSA-NCAM in postnatal brain development. It is therefore unlikely that NCAM-EC$^{tg}$ perturbs interneuronal synapses by decreasing NCAM interactions due to polysialylation.

### Impaired branching of cortical basket interneurons in developing NCAM-EC transgenic brain

To examine the effects of NCAM-EC overexpression on differentiation of basket interneurons in the PFC, NCAM-EC transgenic mice were intercrossed with a BAC transgenic strain that expresses enhanced green fluorescent protein (EGFP) from the GAD67 promoter in a subpopulation of basket cells (Chattopadhyaya 2004). We focused on the anterior cingulate cortex, as it has important functions in working memory and may be analogous to the human dorsolateral prefrontal cortex (DLPFC) (Kuroda 1998; Lewis 2005). Basket cells from the PFC of GAD67-EGFP or NCAM-EC/GAD67-EGFP mice (matched for rostrocaudal level) were subjected to confocal imaging, then reconstructed from confocal z-stacks using Neurolucida software (4−5 animals per genotype per stage, 30−50 neurons per mouse). Mice were analyzed at P10 (neonatal), P20 (approaching adolescence) and 5 months (adult). Analysis was restricted to an area 30 μm proximal to the neuronal soma, as branching was difficult to trace more distally in confocal z-stacks. Although basket cells have extensive axonal arbors that target pyramidal soma in multiple cortical layers and columns (distal branching), they exhibit elaborate local branching that is important in regulation of neighboring pyramidal neurons (Huang 2007). WT GAD67-EGFP basket cells elaborated primary processes (axons and dendrites emerging from the soma) by P10, and developed extensively branched arbors from P20 to adult (typical neurons are shown in each panel of Fig. 2). NCAM-EC basket cells showed similar process

initiation at P10, but exhibited obvious stunting of process arborization at P20 and adult (Fig. 2). Quantitation of basket cell arborization revealed that the branching index of WT basket cells increased from P10 to P20 (Fig. 3A, $p<0.05$), whereas the branching index of NCAM-EC basket cells did not increase with development and was significantly less than WT at P20 and adult (Fig. 3A, $p<0.05$). Similar results were obtained by Sholl analysis, which measures the number of times a branched neuronal process crosses a concentric circle at a given distance from the soma. The number of process crossings of WT basket cells increased from P10 to P20 at a Sholl distance of 20 μm from the soma (Fig. 3B, $p<0.05$), with a slight decrease in the adult. In NCAM-EC basket cells, the number of process crossings was significantly less than WT at P20 and adult ($p<0.05$). Similar results were seen at a Sholl distance of 10 μm (not shown).

Underdevelopment of proximal branching of basket interneurons in the NCAM-EC PFC was not attributed to fewer primary processes, as there was no significant difference in the number of processes between genotypes at any age (Fig. 3C). Furthermore, neuronal density was unchanged at each stage (Fig. 3D). Likewise, somal area (Fig. 3E), which is known to decrease during apoptosis, did not vary between genotypes at any stage. Taken together, these data showed that basket cell processes are impaired in their proximal arborization in the presence of excessive soluble NCAM-EC at postnatal stages approaching adolescence.

## Development of perisomatic synapses of basket cell axons is impaired in NCAM-EC PFC

A major period of synaptic development of basket cells takes place at postnatal stages corresponding to adolescence in the mouse visual cortex (P20 – P36; reviewed in (Huang 2007)). To analyze the development of perisomatic innervation by basket cells in the PFC, and to determine if the reduced branching of these interneurons resulting from NCAM-EC overexpression might lead to reduced synapses, perisomatic synaptic puncta (Esclapez 1994) arising from GAD67-EGFP basket cells were examined in WT and NCAM-EC PFC at P10, P20 and adult (5 month) stages. In WT and NCAM-EC PFC, fluorescent synaptic puncta of basket cells surrounding soma were seen to increase from relatively low levels at P10-P20 to higher levels in adult (Fig. 4). In NCAM-EC transgenic PFC, perisomatic puncta appeared to be decreased compared to WT PFC at both P20 and adult. Quantitative measurement of fluorescent pixel density of puncta rings surrounding the soma showed that in WT PFC, perisomatic fluorescent puncta rings increased approximately 3-fold from P10 to adult, whereas in NCAM-EC PFC puncta were significantly decreased at P20 and adult (Fig. 4A, B).

The 65 kDa isoform of glutamic acid decarboxylase (GAD65) is enriched in nerve terminals of GABAergic inhibitory neurons, where it can be activated during high GABA demand (Feldblum, 1993; Esclapez, 1994). As an additional marker for development of GABAergic synaptic terminals, GAD65 expression was examined in WT and NCAM-EC PFC by immunofluorescence staining. In WT PFC, perisomatic GAD65-positive immunofluorescence increased from P10 to P20 and remained elevated in adult ($p<0.05$; Fig. 5A, B). In NCAM-EC mice, GAD65-positive perisomatic puncta were significantly lower than WT at P20 and in adult (Fig. 5B, $p<0.01$). These results were in accord with the observed decrease in perisomatic puncta of GAD67-EGFP-labeled basket cells during the adolescent to adult transition (Fig. 4). The decrease in GAD65-positive puncta in NCAM-EC compared to WT PFC was much greater than that of GAD67-EGFP-labeled basket cell puncta, consistent with the possibility that other subclasses of basket cells or types of GABAergic interneurons might also be impaired for synaptic development and/or branching by overexpression of NCAM-EC.

## Synaptophysin-positive synapses in PFC are impaired by NCAM-EC overexpression

To investigate whether synaptic development was impaired more globally by NCAM-EC overexpression, WT and NCAM-EC PFC was examined at P10, P20 and adult stages for

expression of the presynaptic terminal marker synaptophysin in perisomatic puncta. Synaptophysin staining should approximate synaptic density, as it is localized in terminals of both interneurons and pyramidal cells. In WT PFC, there was little difference in synaptophysin-positive perisomatic puncta at any postnatal stage. This was consistent with findings that a large proportion of pyramidal neuron synaptic development takes place by the time of birth in mouse (reviewed in (McAllister 2007)), although additional synapses form and are remodeled during adolescence (P20) as a consequence of activity-dependent plasticity (Antonini and Stryker 1993). By contrast, in NCAM-EC PFC there were significant decreases in synaptophysin-positive perisomatic puncta compared to WT at P20 and adult (Fig. 6B). In part, the decrease in synaptophysin-positive puncta from NCAM-EC PFC may be attributed to reduced interneuron synapses. However, the large majority of cortical synapses are excitatory (deFelipe, 2002) and only ~25% of neurons in the mammalian brain are interneurons (Markram 2004), thus the greater decrease in synaptophysin-positive puncta (~70%) compared to GAD65-positive puncta (58%) in NCAM-EC PFC compared to WT suggest that excitatory synapses were likely to be impaired by NCAM-EC expression.

### Soluble NCAM-EC inhibits NCAM-dependent neurite growth and branching

To determine if diffusible, exogenous NCAM-EC impairs WT axonal/dendritic growth and branching by blocking NCAM-dependent interactions, embryonic cortical neurons from WT E16.5 mice were plated onto monolayers of L-fibroblasts or NCAM140 expressing L-fibroblasts (Beggs 1994; Hinkle 2006). Neurites were allowed to extend for 72 h in the absence (nonimmune IgG) or presence of purified soluble NCAM extracellular domain fused to the Fc portion of human IgG (NCAM-Fc, 50 μg/ml). This high dose of NCAM-Fc was used to mimic the overexpression or dysregulated shedding of NCAM found in the NCAM-EC transgenic mouse. Neuronal processes were visualized using antibodies for neuron-specific βIII tubulin (TUJ1, (Ferreira and Caceres 1992)). Data from a representative experiment is shown in Figure 7. In the presence of nonimmune IgG, neurons plated onto L-fibroblasts extended short, relatively unbranched neurites, while those plated onto NCAM140-expressing L-fibroblasts extended long, branched neurites (Fig. 7A). In these cultures, the percent of neurons with branched neurites on NCAM increased almost 2-fold, while neurite outgrowth on NCAM increased 1.8-fold (Fig. 7B,C, $p<0.05$), similar to previous results (Hinkle 2006). In the presence of NCAM-Fc fusion protein, neurons growing on L-fibroblasts, had neurites similar in branching and length to those treated with nonimmune IgG (Fig. 7A, B, C). In contrast, neurons growing on NCAM140-expressing L-fibroblasts in the presence of NCAM-Fc exhibited only short, unbranched neurites and resembled neurons on L-fibroblasts not expressing NCAM (Fig. 7A). In the presence of NCAM-Fc, neurons on NCAM-expressing fibroblasts showed branching and outgrowth that was ~50% the level of neurons treated with nonimmune IgG (Fig. 7B, C, $p<0.005$). Cortical neurons from NCAM-EC mice show reduced NCAM-dependent neurite growth and branching *in vitro* (Hinkle 2006), suggesting that soluble NCAM-EC may interfere with homophilic and/or heterophilic NCAM interactions. As NCAM-EC is produced locally by each individual neuron, this effect may be due to impaired neurite initiation or attachment to the substrate. Although NCAM-EC neurons extend neurites less frequently than WT neurons (Hinkle 2006), there was no significant difference in the number of WT neurons extending neurites after treatment with NCAM-Fc. Thus, the reduction in neurite growth and branching by exogenous NCAM-EC supports a mechanism in which soluble NCAM-EC blocks NCAM-dependent interactions required for growth and branching of cortical neurons in development.

## DISCUSSION

Here, we have studied NCAM-EC transgenic mice to examine the developmental mechanisms that control the impairment in neuronal connectivity resulting from overexpression of the

soluble NCAM extracellular domain (NCAM-EC). GABAergic basket cells in WT PFC displayed progressive neuronal arborization and formation of perisomatic synapses concomitant with loss of polysialylation during the postnatal transition to adolescence (P10-P20). In striking contrast, basket cell arborization and synaptogenesis in the NCAM-EC PFC did not progress past the P10 stage, suggesting that overexpression of soluble NCAM-EC perturbs the postnatal development of basket interneurons resulting in decreased synaptic connectivity. In cultures of primary cortical neurons, soluble NCAM-EC fusion protein inhibited branching and outgrowth of neurites, supporting an inhibitory function for the NCAM-EC fragment. The results are consistent with a dominant inhibitory mechanism in which overexpression of NCAM-EC perturbs axonal/dendritic branching of basket interneurons at adolescence, resulting in reduced perisomatic innervation of cortical neurons.

NCAM-EC protein in transgenic mice was found to be expressed throughout postnatal mouse brain development as a non-polysialylated species. In addition, the expression of NCAM-EC had no effect on endogenous NCAM polysialylation (Fig. 1B) or on NCAM isoform expression (Pillai-Nair 2005). Because the transgenic NCAM-EC protein did not contain PSA, its effect on NCAM-dependent neurite outgrowth and synaptogenesis could not be ascribed to the well-documented loss of NCAM affinity due to polysialylation (Rutishauser 1988; Johnson 2005). More likely, the developmental decrease in axonal/dendritic branching and synaptogenesis in the NCAM-EC$^{tg}$ PFC is caused by competitive interaction of soluble NCAM-EC fragments with transmembrane NCAM acting to inhibit homo- or heterophilic interactions during postnatal development of the brain. This idea is in accord with evidence that NCAM-NCAM interactions mediate terminal branching and synapse stability or maturation (Jorgensen 1995; Schuster 1998; Dityatev 2000; Cambon 2004; Landmesser 2007).

NCAM in normal mouse brain was predominantly expressed in its polysialylated form from E18.5-P10, corresponding to major stages of neuronal differentiation and axonal/dendritic growth. Thereafter, in the adolescent transition, PSA-NCAM was converted to the major transmembrane isoforms of NCAM180 and NCAM140, potentially enabling synapses to form, in accord with others (Edelman and Chuong 1982; Galuska 2007). Proteolytic cleavage of NCAM in embryonic cortical neurons in culture produces NCAM-EC and a residual intracellular cytoplasmic domain fragment generated by the activation of an ADAM-type metalloprotease requiring ERK MAP kinase activity (Diestel 2005; Hubschmann 2005; Hinkle 2006; Kalus 2006). NCAM fragments corresponding in size to the extracellular region were present in normal mouse brain from E18.5-P10, suggesting that NCAM is normally regulated by limited proteolytic cleavage of the ectodomain during stages of axonal/dendritic growth. The sizes of NCAM soluble extracellular (105−110 kDa) cleavage fragments were identical to those previously observed in rat brain, cerebrospinal fluid, and cultured mouse cortical and hippocampal neurons (Krog 1992; Buttner 2004; Diestel 2005; Hubschmann 2005; Hinkle 2006; Kalus 2006) and appeared to be derived from nonpolysialylated NCAM. However, it cannot be ruled out that PSA-NCAM is also subject to shedding and more rapidly degraded. We were unable to detect the NCAM-ICD cleavage fragment at any stage, consistent with rapid turnover.

A limitation of this study is that many basket cells are labeled in the PFC of GAD67-EGFP mice and their arbors extensively overlap, precluding analysis of the distal arbor of the fluorescent cells. Moreover, we have not identified other interneuronal subtypes that may contribute to the NCAM-Fc-mediated reductions in branching and outgrowth of GAD65-positive interneurons, which was suggested by the greater decrease in GAD65-positive puncta than in GAD67-EGFP-labeled basket cells in NCAM-EC transgenic PFC. Synaptophysin-positive synapses were also reduced significantly during synaptogenesis and adult stages in NCAM-EC mice. Taken together with previous studies in adult NCAM-EC mice showing that

the number of apical dendritic spines are decreased (Pillai-Nair 2005), our results suggest that pyramidal neuron development is also impaired by NCAM-EC overexpression.

In other systems, low concentrations of soluble NCAM-Fc (5 μg/ml) acts as a substrate to promote the neurite growth of hippocampal neurons (Bodrikov 2005; Santuccione 2005) and cerebellar granule cells (Meiri 1998). The higher concentrations of NCAM-Fc used here mimic the increased levels of soluble NCAM-EC in the transgenic mouse which inhibit interneuron branching *in vivo.* Furthermore, the lower levels of NCAM-EC present at P10 may mimic the lower concentrations previously described (Meiri 1998; Bodrikov 2005; Santuccione 2005) to promote outgrowth. However, this had no promoting effect on interneuron development *in vivo*. Furthermore, the apparent discrepancy in the neurite outgrowth promoting ability of NCAM-Fc may lie in cell type specific responses to the protein. As we previously described, metalloprotease-induced ectodomain shedding blocks NCAM-dependent neurite growth and branching from cortical neurons (Hinkle 2006), while the same phenomenon increases outgrowth from hippocampal neurons (Hubschmann 2005; Kalus 2006). Thus, cortical neurons may be more sensitive to inhibitory actions of soluble NCAM than other neuronal types.

Analysis of basket cell development in the NCAM-EC transgenic mouse model supports a mechanism in which the NCAM-EC cleavage fragment acts as an inhibitor of cortical interneuronal arborization resulting in diminished synaptic development (Figure 8). Excess soluble NCAM-EC, could interact with increasing levels of non-polysialylated NCAM on developing neurons, disrupting NCAM homophilic and heterophilic interactions and signaling (Meiri 1998; Schmid 1999; Kolkova 2000; Niethammer 2002; Bodrikov 2005; Santuccione 2005). Our studies show that NCAM-EC strikingly decreases axonal/dendritic arborization of basket cells, and potentially other interneurons, thus reducing the number of perisomatic synapses in the PFC. In normal interneuron development, NCAM cleavage during stages of axonal/dendritic outgrowth may serve a regulatory role. As a result of an outside stimulus leading to ERK activation, an ADAM family metalloprotease is stimulated to cleave NCAM, which may limit branching of interneuronal arbors, allowing inhibitory synapses to form in appropriate numbers. The results presented here provide novel insight on potential mechanisms underlying disease states, such as schizophrenia, in which NCAM dysregulation is implicated.

**ACKNOWLEDGMENTS**

We would like to thank Dr. Neeta Pillai-Nair for assistance in obtaining images for basket cell morphology, Dr. John Gilmore for providing use of the Neurolucida software and for productive discussions. This work was supported by the UNC Schizophrenia Research Center, an NIMH Silvio O. Conte Center for the Neuroscience of Mental Disorders, (NIH grant MH064065 P.F.M.).

## Abbreviations

NCAM, neural cell adhesion molecule
NCAM-EC, NCAM extracellular domain
NCAM-EC$^{tg}$, NCAM-EC transgenic protein
LTP, long-term potentiation
WT, wild-type
SNP, single nucleotide polymorphism
PSA, polysialic acid
PFC, prefrontal cortex
PPI, prepulse inhibition of acoustic startle
EGFP, enhanced green fluorescent protein
PMSF, phenylmethylsulfonylfluoride
HA, hemagglutinin
FBS, fetal bovine serum

ADAM, a disintegrin and metalloprotease

## REFERENCES


Aizenman CD, Huang EJ, Linden DJ. Morphological correlates of intrinsic electrical excitability in neurons of the deep cerebellar nuclei. J Neurophysiol 2003;89:1738–47. [PubMed: 12686564]

Angata K, Fukuda M. Polysialyltransferases: major players in polysialic acid synthesis on the neural cell adhesion molecule. Biochimie 2003;85:195–206. [PubMed: 12765789]

Antonini A, Stryker MP. Rapid remodeling of axonal arbors in the visual cortex. Science 1993;260:1819–1821. [PubMed: 8511592]

Arai M, Yamada K, Toyota T, Obata N, Haga S, Yoshida Y, Nakamura K, Minabe Y, Ujike H, Sora I, Ikeda K, Mori N, Yoshikawa T, Itokawa M. Association between polymorphisms in the promoter region of the sialyltransferase 8B (SIAT8B) gene and schizophrenia. Biol Psychiatry 2006;59:652–659. [PubMed: 16229822]

Barbeau D, Liang JJ, Robitalille Y, Quirion R, Srivastava LK. Decreased expression of the embryonic form of the neural cell adhesion molecule in schizophrenic brains. Proc Natl Acad Sci USA 1995;92:2785–2789. [PubMed: 7708724]

Beggs HE, Soriano P, Maness PF. NCAM-dependent neurite outgrowth is inhibited in neurons from *fyn*-minus mice. J Cell Biol 1994;127:825–833. [PubMed: 7962063]

Bock E, Edvardsen K, Gibson A, Linnemann D, Lyles JM, Nybroe O. Characterization of soluble forms of NCAM. FEBS Lett 1987;225:33–36. [PubMed: 2446924]

Bodrikov V, Leshchyns'ka I, Sytnyk V, Overvoorde J, den Hertog J, Schachner M. RPTPalpha is essential for NCAM-mediated p59fyn activation and neurite elongation. J Cell Biol 2005;168:127–39. [PubMed: 15623578]

Brocco MA, Frasch AC. Interfering polysialyltransferase ST8SiaII/STX mRNA inhibits neurite growth during early hippocampal development. FEBS Lett 2006;580:4723–6. [PubMed: 16887122]

Bruses JL, Rutishauser U. Roles, regulation, and mechanism of polysialic acid function during neural development. Biochimie 2001;83:635–43. [PubMed: 11522392]

Bukalo O, Fentrop N, Lee AY, Salmen B, Law JW, Wotjak CT, Schweizer M, Dityatev A, Schachner M. Conditional ablation of the neural cell adhesion molecule reduces precision of spatial learning, long-term potentiation, and depression in the CA1 subfield of mouse hippocampus. J Neurosci 2004;24:1565–1577. [PubMed: 14973228]

Buttner B, Reutter W, Horstkorte R. Cytoplasmic domain of NCAM 180 reduces NCAM-mediated neurite outgrowth. J Neurosci Res 2004;75:854–860. [PubMed: 14994346]

Cambon K, Hansen SM, Venero C, Herrero AI, Skibo G, Berezin V, Bock E, Sandi C. A synthetic neural cell adhesion molecule mimetic peptide promotes synaptogenesis, enhances presynaptic function, and facilitates memory consolidation. J Neurosci 2004;24:4197–4204. [PubMed: 15115815]

Chattopadhyaya B, Di Cristo G, Higashiyama H, Knott GW, Kuhlman SJ, Welker E, Huang ZJ. Experience and activity-dependent maturation of perisomatic GABAergic innervation in primary visual cortex during a postnatal critical period. J Neurosci 2004;24:9598–9611. [PubMed: 15509747]

Conchonaud F, Nicolas S, Amoureux MC, Menager C, Marguet D, Lenne PF, Rougon G, Matarazzo V. Polysialylation increases lateral diffusion of neural cell adhesion molecule in the cell membrane. J Biol Chem 2007;282:26266–74. [PubMed: 17623676]

Cremer H, Chazal G, Carleton A, Goridis C, Vincent JD, Lledo PM. Long-term but not short-term plasticity at mossy fiber synapses is impaired in neural cell adhesion molecule-deficient mice. Proc Natl Acad Sci U S A 1998;95:13242–13247. [PubMed: 9789073]

Cremer H, Chazal G, Goridis C, Represa A. NCAM is essential for axonal growth and fasciculation in the hippocampus. Mol Cell Neurosci 1997;8:323–335. [PubMed: 9073395]

Cremer H, Lange R, Christoph A, Plomann M, Vopper G, Roes J, Brown R, Baldwin S, Barthels D, Rajewsky K, Wille W. Inactivation of the N-CAM gene in mice results in size reduction of the olfactory bulb and deficits in spatial learning. Nature 1994;367:455–459. [PubMed: 8107803]

Demyanenko G, Tsai A, Maness PF. Abnormalities in neuronal process extension, hippocampal development, and the ventricular system of L1 knockout mice. J Neurosci 1999;19:4907–4920. [PubMed: 10366625]

di Cristo, G.; Chattopadhyaya, B.; Kuhlman, SJ.; Wu, CZ.; Rutishauser, U.; Maffei, L.; Huang, JZ. Activity-dependent down regulation of PSA-NCAM promotes the maturation of GABAergic innervation and the onset of critical period plasticity in visual cortex; 3rd International polySia Meeting; Bad Lauterberg, Germany. 2007.

Diestel S, Hinkle CL, Schmitz B, Maness PF. NCAM140 stimulates integrin-dependent cell migration by ectodomain shedding. J Neurochem 2005;95:1777–84. [PubMed: 16277615]

Dityatev A, Dityateva G, Schachner M. Synaptic strength as a function of post-versus presynaptic expression of the neural cell adhesion molecule NCAM. Neuron 2000;26:207–217. [PubMed: 10798405]

Edelman GM, Chuong CM. Embryonic to adult conversion of neural cell adhesion molecules in normal and staggerer mice. Proc Natl Acad Sci USA 1982;79:7036–7040. [PubMed: 6960362]

Esclapez M, Tillakaratne NJ, Kaufman DL, Tobin AJ, Houser CR. Comparative localization of two forms of glutamic acid decarboxylase and their mRNAs in rat brain supports the concept of functional differences between the forms. J Neurosci 1994;14:1834–1855. [PubMed: 8126575]

Ferreira A, Caceres A. Expression of the class III beta-tubulin isotype in developing neurons in culture. J Neurosci Res 1992;32:516–529. [PubMed: 1527798]

Flames N, Long JE, Garratt AN, Fischer TM, Gassmann M, Birchmeier C, Lai C, Rubenstein JL, Marin O. Short- and long-range attraction of cortical GABAergic interneurons by neuregulin-1. Neuron 2004;44:251–261. [PubMed: 15473965]

Galuska, SP.; Oltmann-Norden, I.; Geyer, H.; Weinhold, B.; Kuchelmeister, K.; Hildebrandt, H.; Gerardy-Schahn, R.; Geyer, R.; Muhlenhoff, M. Impact of the two polysialyltransferases ST8SiaII and ST8SiaIV on the polysialic acid pattern in mouse brain; 3rd International polySia Meeting; Bad Lauterberg, Germany. 2007.

Gascon E, Vutskits L, Kiss JZ. Polysialic acid-neural cell adhesion molecule in brain plasticity: From synapses to integration of new neurons. Brain Res Rev. 2007

Hinkle CL, Diestel S, Lieberman J, Maness PF. Metalloprotease-induced ectodomain shedding of neural cell adhesion molecule (NCAM). Journal of Neurobiology 2006;66:1378–95. [PubMed: 16967505]

Hinkle, CL.; Maness, PF. Regulation of neural cell adhesion molecule function by ectodomain shedding.. In: Pandalai, SG., editor. Recent Research Developments in Molecular and Cellular Biology. 6. Research Signpost.; Kerala, India: 2006. p. 121-136.

Huang ZJ, Di Cristo G, Ango F. Development of GABA innervation in the cerebral and cerebellar cortices. Nat Rev Neurosci 2007;8:673–86. [PubMed: 17704810]

Huang ZJ, Kirkwood A, Pizzorusso T, Porciatti V, Morales B, Bear MF, Maffei L, Tonegawa S. BDNF regulates the maturation of inhibition and the critical period of plasticity in mouse visual cortex. Cell 1999;98:739–755. [PubMed: 10499792]

Hubschmann MV, Skladchikova G, Bock E, Berezin V. Neural cell adhesion molecule function is regulated by metalloproteinase-mediated ectodomain release. J Neurosci Res 2005;80:826–837. [PubMed: 15884014]

Johnson CP, Fujimoto I, Rutishauser U, Leckband DE. Direct evidence that NCAM polysialylation increases intermembrane repulsion and abrogates adhesion. J Biol Chem 2005;280:137–145. [PubMed: 15504723]

Jorgensen OS. Neural cell adhesion molecule (NCAM) as a quantitative marker in synaptic remodeling. Neurochem Res 1995;20:533–47. [PubMed: 7643959]

Kalus I, Bormann U, Mzoughi M, Schachner M, Kleene R. Proteolytic cleavage of the neural cell adhesion molecule by ADAM17/TACE is involved in neurite outgrowth. J Neurochem 2006;98:78–88. [PubMed: 16805798]

Kiselyov VV, Skladchikova G, Hinsby AM, Jensen PH, Kulahin N, Soroka V, Pedersen N, Tsetlin V, Poulsen FM, Berezin V, Bock E. Structural basis for a direct interaction between FGFR1 and NCAM and evidence for a regulatory role of ATP. Structure (Camb) 2003;11:691–701. [PubMed: 12791257]

Kiselyov VV, Soroka V, Berezin V, Bock E. Structural biology of NCAM homophilic binding and activation of FGFR. J Neurochem 2005;94:1169–79. [PubMed: 16045455]

Kolkova K, Novitskaya V, Pedersen N, Berezin V, Bock E. Neural cell adhesion molecule-stimulated neurite outgrowth depends on activation of protein kinase C and the Ras-mitogen-activated protein kinase pathway. J Neurosci 2000;20:2238–2246. [PubMed: 10704499]

Kondoh M, Shiga T, Okado N. Regulation of dendrite formation of Purkinje cells by serotonin through serotonin1A and serotonin2A receptors in culture. Neurosci Res 2004;48:101–9. [PubMed: 14687886]

Krog L, Olsen M, Dalseg AM, Roth J, Bock E. Characterization of soluble neural cell adhesion molecule in rat brain, CSF, and plasma. J Neurochem 1992;59:838–847. [PubMed: 1494910]

Kuroda M, Yokofujita J, Murakami K. An ultrastructural study of the neural circuit between the prefrontal cortex and the mediodorsal nucleus of the thalamus. Prog Neurobiol 1998;54:417–58. [PubMed: 9522395]

Landmesser, L.; Polo-Parada, L.; Maeno-Hikichi, Y.; Katsusuke, H. Novel roles of NCAM isoforms in synaptic maturation and transmission; 3rd International polySia meeting; Bad Lauterberg, Germany. 2007.

Lauder JM, Han VK, Henderson P, Verdoorn T, Towle AC. Prenatal ontogeny of the GABAergic system in the rat brain: an immunocytochemical study. Neuroscience 1986;19:465–493. [PubMed: 3022187]

Lewis DA, Hashimoto T, Volk DW. Cortical inhibitory neurons and schizophrenia. Nat Rev Neurosci 2005;6:312–324. [PubMed: 15803162]

Lyons F, Martin ML, Maguire C, Jackson A, Regan CM, Shelley RK. The expression of an N-CAM serum fragment is positively correlated with severity of negative features in type II schizophrenia. Biol Psychiatry 1988;23:769–775. [PubMed: 3365455]

Maness PF, Schachner M. Neural recognition molecules of the immunoglobulin superfamily: signaling transducers of axon guidance and neuronal migration. Nat Neurosci 2007;10:19–26. [PubMed: 17189949]

Markram H, Toledo-Rodriguez M, Wang Y, Gupta A, Silberberg G, Wu C. Interneurons of the neocortical inhibitory system. Nat Rev Neurosci 2004;5:793–807. [PubMed: 15378039]

McAllister AK. Dynamic aspects of CNS synapse formation. Annu Rev Neurosci 2007;30:425–50. [PubMed: 17417940]

Meiri KF, Saffell JL, Walsh FS, Doherty P. Neurite outgrowth stimulated by neural cell adhesion molecules requires growth-associated protein-43 (GAP-43) function and is associated with GAP-43 phosphorylation in growth cones. J Neurosci 1998;18:10429–10437. [PubMed: 9852580]

Nakayama J, Angata K, Ong E, Katsuyama T, Fukuda M. Polysialic acid, a unique glycan that is developmentally regulated by two polysialyltransferases, PST and STX, in the central nervous system: from biosynthesis to function. Pathol Int 1998;48:665–77. [PubMed: 9778105]

Niethammer P, Delling M, Sytnyk V, Dityatev A, Fukami K, Schachner M. Cosignaling of NCAM via lipid rafts and the FGF receptor is required for neuritogenesis. J Cell Biol 2002;157:521–532. [PubMed: 11980923]

Nybroe O, Linnemann D, Bock E. Heterogeneity of soluble neural cell adhesion molecule. J Neurochem 1989;53:1372–1378. [PubMed: 2795005]

Pillai-Nair N, Panicker AK, Rodriguiz RM, Gilmore KL, Demyanenko GP, Huang JZ, Wetsel WC, Maness PF. Neural cell adhesion molecule-secreting transgenic mice display abnormalities in GABAergic interneurons and alterations in behavior. J Neurosci 2005;25:4659–4671. [PubMed: 15872114]

Polleux F, Ghosh A. The slice overlay assay: a versatile tool to study the influence of extracellular signals on neuronal development. Sci STKE 2002;2002:L9.

Polo-Parada L, Bose CM, Landmesser LT. Alterations in transmission, vesicle dynamics, and transmitter release machinery at NCAM-deficient neuromuscular junctions. Neuron 2001;32:815–828. [PubMed: 11738028]

Rutishauser U, Acheson A, Hall AK, Mann DM, Sunshine J. The neural cell adhesion molecule (NCAM) as a regulator of cell-cell interactions. Science 1988;240:53–7. [PubMed: 3281256]

Santuccione A, Sytnyk V, Leshchyns'ka I, Schachner M. Prion protein recruits its neuronal receptor NCAM to lipid rafts to activate p59fyn and to enhance neurite outgrowth. J Cell Biol 2005;169:341–54. [PubMed: 15851519]

Schmid R-S, Graff R, Schaller MD, Chen S, Schachner M, Hemperley JJ, Maness PF. NCAM Stimulates the Ras-MAPK Pathway and CREB Phosphorylation in Neuronal Cells. J Neurobiol 1999;38:542–555. [PubMed: 10084688]

Schuster T, Krug M, Hassan H, Schachner M. Increase in proportion of hippocampal spine synapses expressing neural cell adhesion molecule NCAM180 following long-term potentiation. J Neurobiol 1998;37:359–372. [PubMed: 9828042]

Spencer KM, Nestor PG, Niznikiewicz MA, Salisbury DF, Shenton ME, McCarley RW. Abnormal neural synchrony in schizophrenia. J Neurosci 2003;23:7407–11. [PubMed: 12917376]

Stoenica L, Senkov O, Gerardy-Schahn R, Weinhold B, Schachner M, Dityatev A. In vivo synaptic plasticity in the dentate gyrus of mice deficient in the neural cell adhesion molecule NCAM or its polysialic acid. Eur J Neurosci 2006;23:2255–64. [PubMed: 16706834]

Stork O, Welzl H, Cremer H, Schachner M. Increased intermale aggression and neuroendocrine response in mice deficient for the neural cell adhesion molecules. Eur J Neurosci 1997;9:424–434. [PubMed: 9104585]

Stork O, Welzl H, Wotjak CT, Hoyer D, Delling M, Cremer H, Schachner M. Anxiety and increased 5-HT1A receptor response in NCAM null mutant mice. J Neurobiol 1999;40:343–355. [PubMed: 10440734]

Sullivan PF, Keefe RS, Lange LA, Lange EM, Stroup TS, Lieberman J, Maness PF. NCAM1 and neurocognition in schizophrenia. Biol Psychiatry 2007;61:902–10. [PubMed: 17161382]

Tao R, Li C, Zheng Y, Qin W, Zhang J, Li X, Xu Y, Shi YY, Feng G, He L. Positive association between SIAT8B and schizophrenia in the Chinese Han population. Schizophr Res 2007;90:108–14. [PubMed: 17126533]

Todaro L, Puricelli L, Gioseffi H, Guadalupe Pallotta M, Lastiri J, Bal de Kier Joffe E, Varela M, Sacerdote de Lustig E. Neural cell adhesion molecule in human serum. Increased levels in dementia of the Alzheimer type. Neurobiol Dis 2004;15:387–393. [PubMed: 15006709]

Ulfig N, Chan WY. Expression Patterns of PSA-NCAM in the Human Ganglionic Eminence and Its Vicinity: Role of PSA-NCAM in Neuronal Migration and Axonal Growth? Cells Tissues Organs 2004;177:229–236. [PubMed: 15459479]

van Kammen DP, Poltorak M, Kelley ME, Yao JK, Gurklis JA, Peters JL, Hemperly JJ, Wright RD, Freed WJ. Further Studies of Elevated Cerebrospinal Fluid Neuroral Cell Adhesion Molecule in Schizophrenia. Biol Psychiatry 1998;43:680–686. [PubMed: 9583002]

Vawter MP. Dysregulation of the neural cell adhesion molecule and neuropsychiatric disorders. Eur J Pharmacol 2000;405:385–395. [PubMed: 11033343]

Vawter MP, Usen N, Thatcher L, Ladenheim B, Zhang P, VanderPutten DM, Conant K, Herman MM, van Kammen DP, Sedvall G, Garver DL, Freed WJ. Characterization of human cleaved N-CAM and association with schizophrenia. Exp Neurol 2001;172:29–46. [PubMed: 11681838]

Vincent SL, Pabreza L, Benes FM. Postnatal maturation of GABA-immunoreactive neurons of rat medial prefrontal cortex. J Comp Neurol 1995;355:81–92. [PubMed: 7636016]

Wang XJ, Tegner J, Constantinidis C, Goldman-Rakic PS. Division of labor among distinct subtypes of inhibitory neurons in a cortical microcircuit of working memory. Proc Natl Acad Sci U S A 2004;101:1368–73. [PubMed: 14742867]

Yelnik J, Percheron G, Francois C. A Golgi analysis of the primate globus pallidus. II. Quantitative morphology and spatial orientation of dendritic arborizations. J Comp Neurol 1984;227:200–13. [PubMed: 6470213]

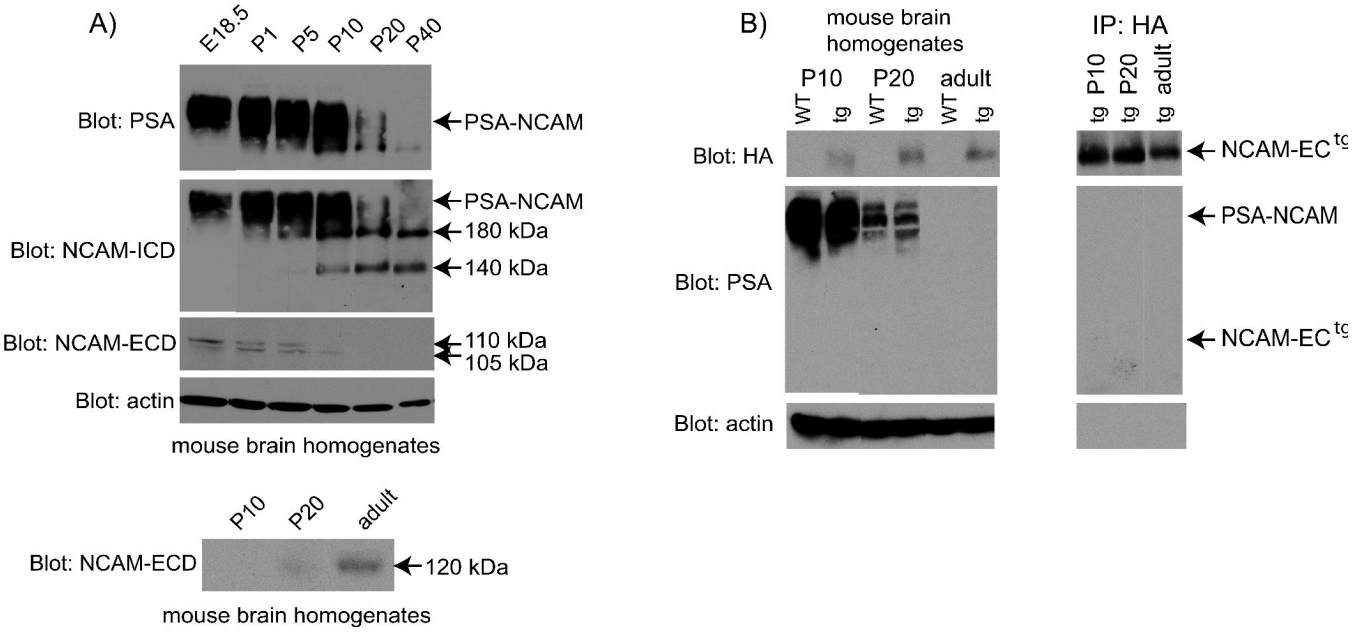


**Figure 1. Expression of different NCAM isoforms and cleavage products during development**

A) NCAM, PSA-NCAM and cleavage fragments during development. Brain homogenates (75 μg) from E18.5 to P40 mice were separated by SDS-PAGE, and blotted using antibodies to PSA (top panel), NCAM-ICD (clone OB11; second panel), and NCAM-ECD (clone H300; third panel). Arrows indicate the size of PSA-NCAM, NCAM180, NCAM140, and cleavage fragments representing the NCAM extracellular domain (105, 110 kDa). NCAM120 expression (bottom panel). Homogenates were blotted using the NCAM-ECD antibody. Actin blots (fourth panel) were used as a loading control. Exposure times were: 1 min (NCAM-ICD, actin), 5 min (PSA, NCAM-ECD bottom panel), 1 h (NCAM-ECD third panel). B) NCAM-$EC^{tg}$ expression and polysialylation. The left set of panels depicts Western blots of mouse brain lysates. For PSA detection, NCAM-$EC^{tg}$ was immunoprecipitated using HA antibodies prior to SDS-PAGE and blots are depicted in the right set of panels. Western blots were performed using antibodies to HA (top panels, 1 min exposure), PSA (middle panels, 5 min exposure), and actin (loading control, bottom panels, 1 min exposure).

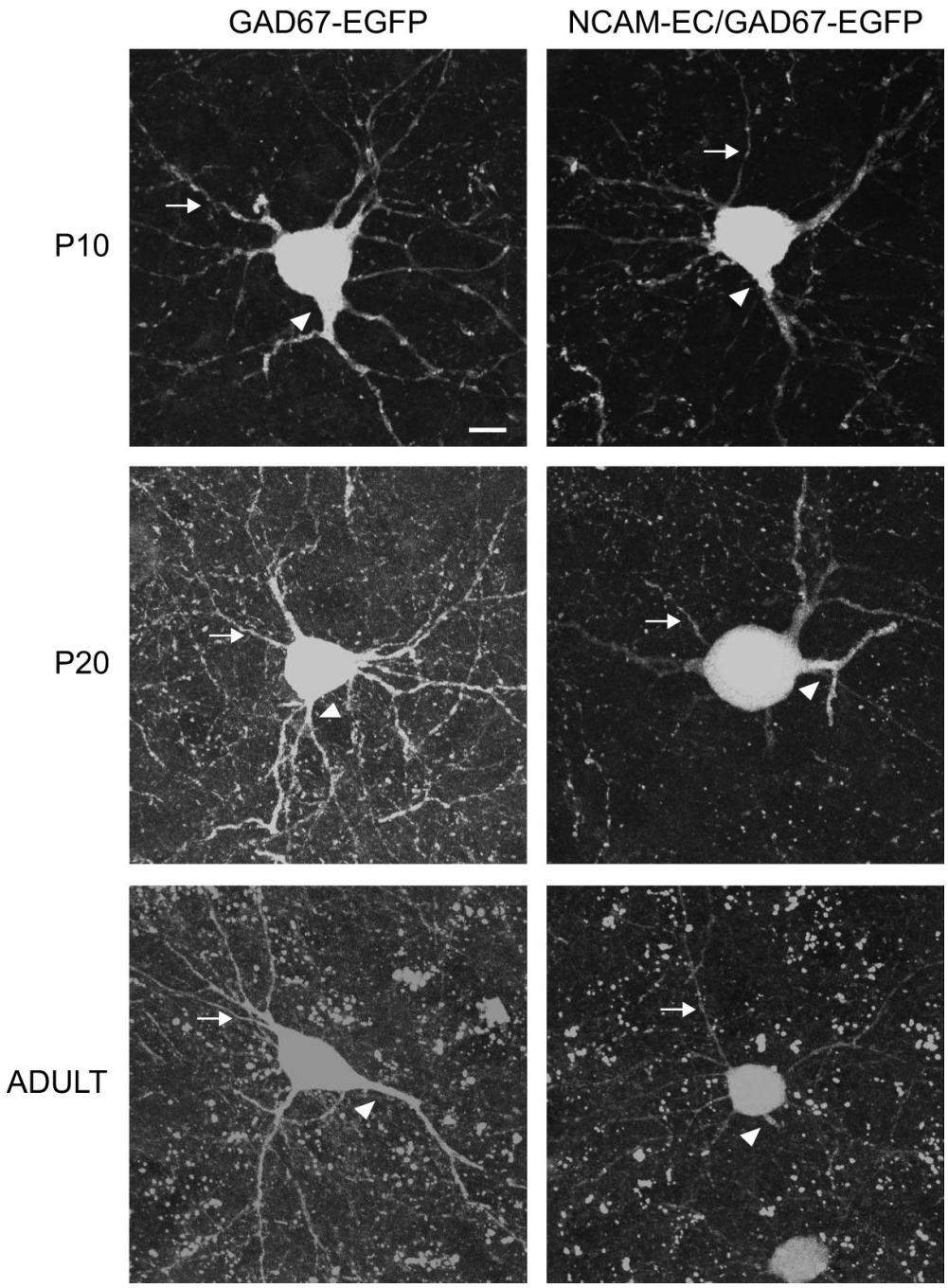


**Figure 2. Development of parvalbumin-positive basket cells in layer II/III of the prefrontal cortex**

Individual neurons from layer II/III of the PFC were imaged and reconstructed using confocal microscopy. Representative extended focus images of individual z-stacks from EGFP-labeled parvalbumin-positive basket cells of WT (GAD67-EGFP) and NCAM-EC transgenic (NCAM-EC/GAD67-EGFP) mice are shown from each time point (P10, P20, adult). Arrows indicate a dendrite in each image. Arrowheads indicate axons. Scale bar = 10 μm.

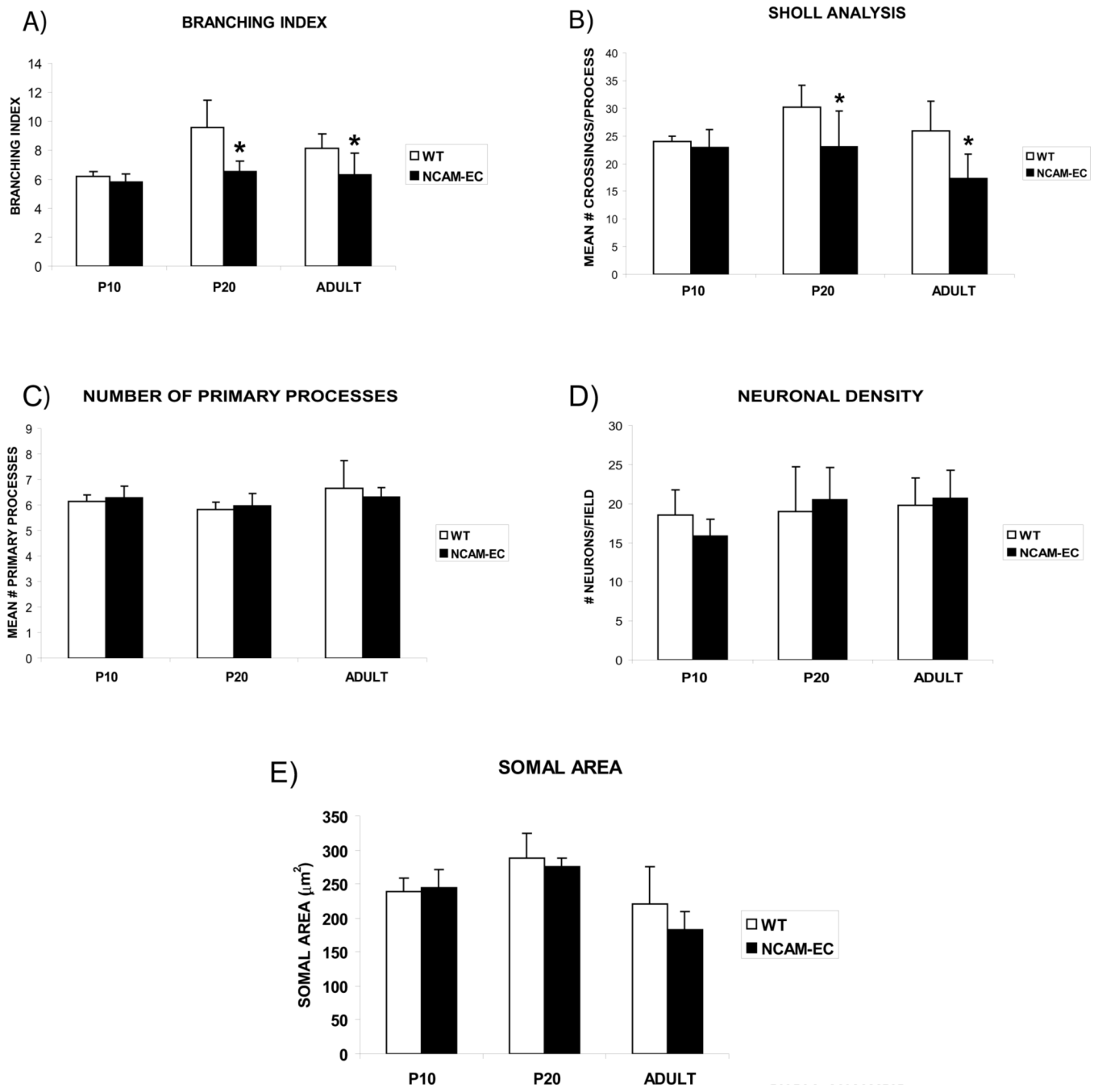


**Figure 3. Proximal neuronal elaboration increases during development, but is stunted in NCAM-EC PFC**

Four to five animals per genotype at P10, P20 and adult were analyzed, and 30−50 neurons per animal were imaged and traced. A) Mean branching index. B) Mean number of crossings per process at a Sholl distance of 20 μm for each time point. Student's t test, *$p<0.05$. C) Mean number of primary processes. D) Mean neuronal density. Five random fields in layer II/III were counted for each animal and averaged. At least 100 neurons were counted per animal. E) Mean somal area ($\mu m^2$).

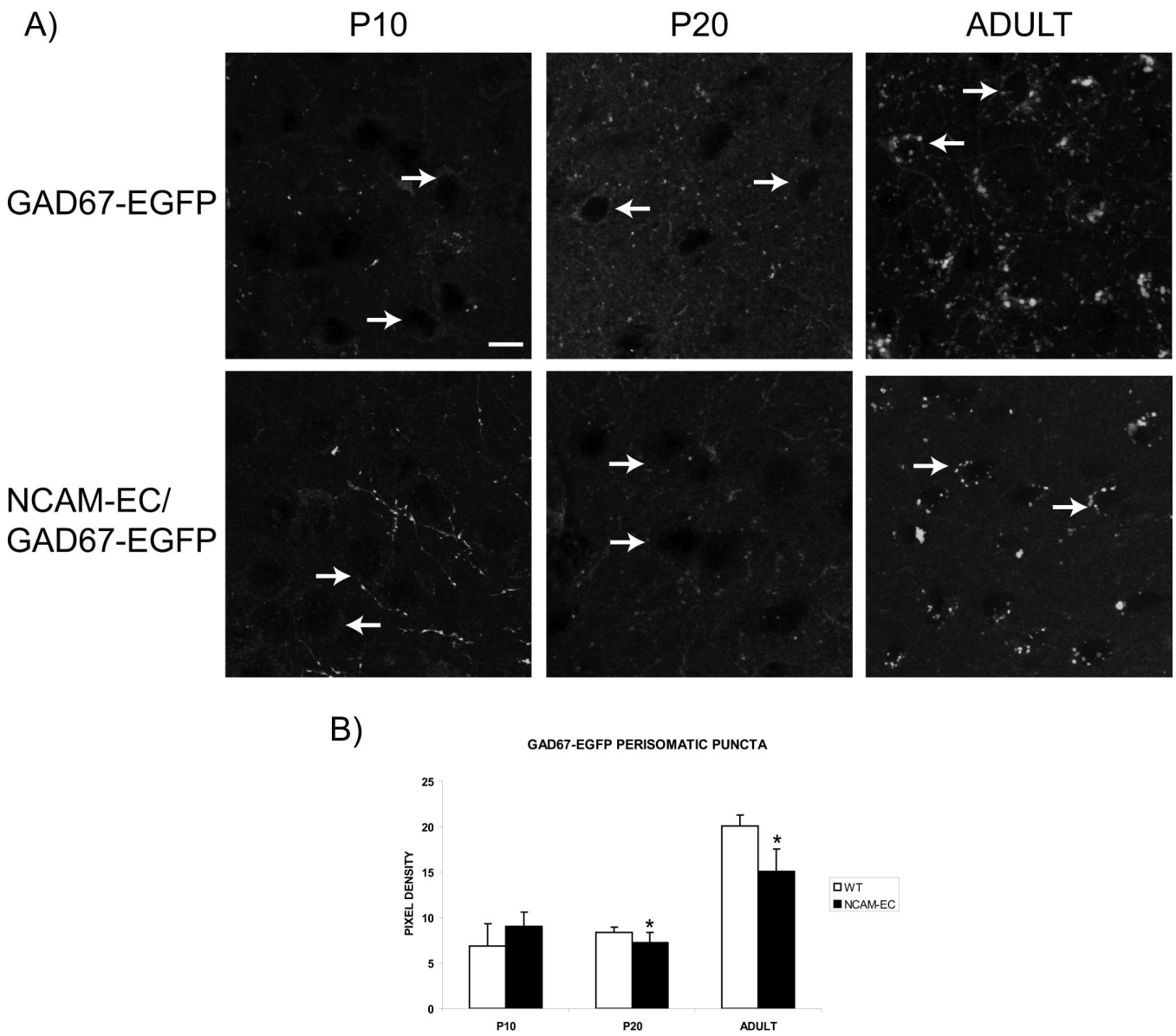


**Figure 4. Perisomatic synapses increase during development, but are reduced in NCAM-ECPFC**

A) Representative images from WT (GAD67-EGFP) and NCAM-EC transgenic (NCAM-EC/GAD67-EGFP) PFC, layer II/III. Scale bar = 10 μm. Arrows indicate the location of representative soma. B) Perisomatic synaptic puncta rings were traced for each image using ImageJ and pixel density measured as compared to the soma as a control. Four images were analyzed for each animal and 4−5 animals per genotype per stage were analyzed. *Student's t test $p<0.05$.

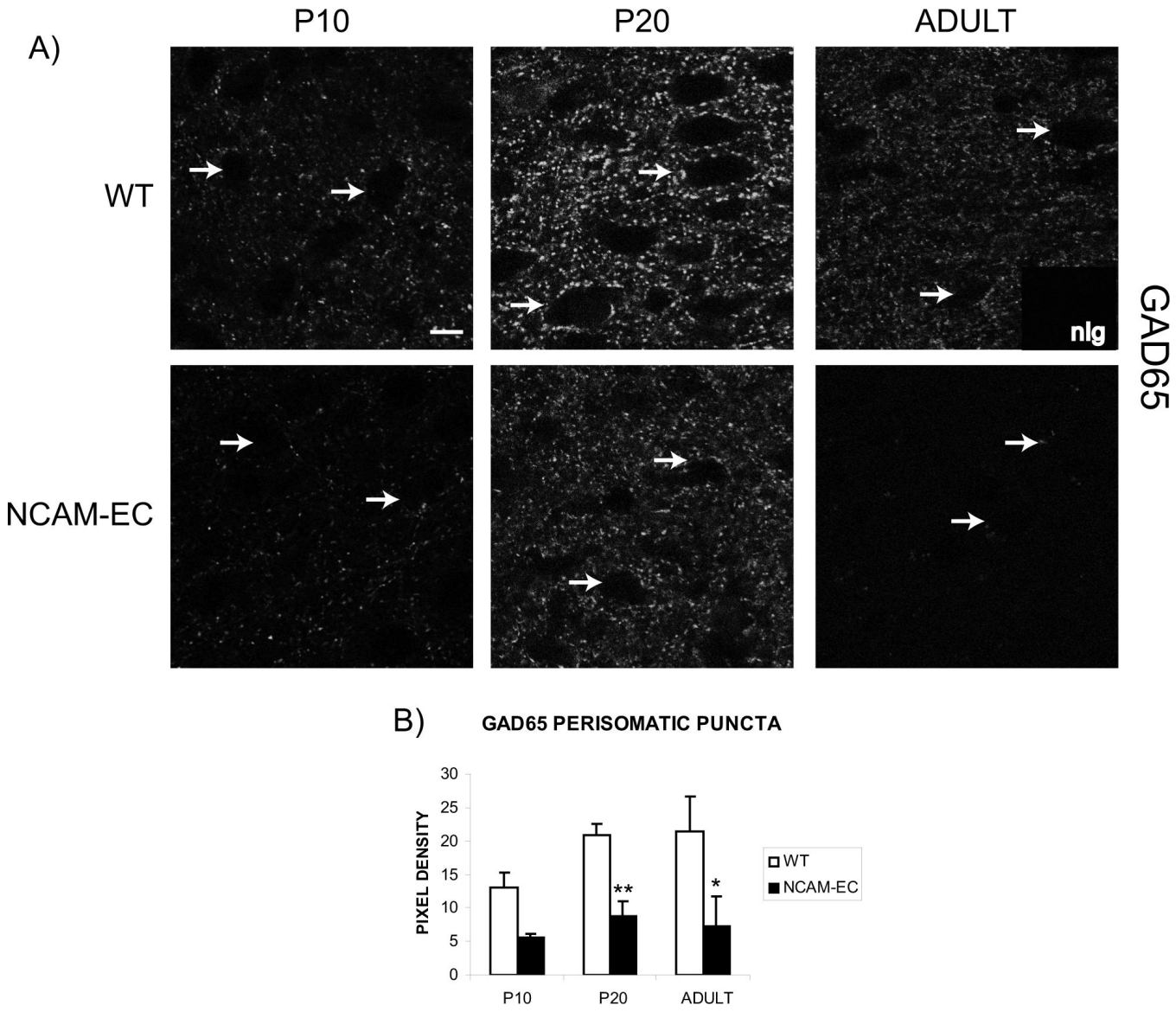


**Figure 5. Synapses from other interneurons develop similarly to parvalbumin-positive basket cells, and are reduced in NCAM-EC mice**

A) Representative images from layer II/III of the PFC of WT and NCAM-EC mice showing GAD65 immunofluorescence. Arrows indicate the location of representative soma. Nonimmune IgG control is shown as an inset. Scale bar = 10 μm. B) Perisomatic synaptic puncta rings were traced for each image using ImageJ and pixel density measured as compared to the soma and nonimmune IgG as a control. Four images were analyzed for each animal and 3 animals per genotype per stage were analyzed. Student's t test **$p<0.005$.

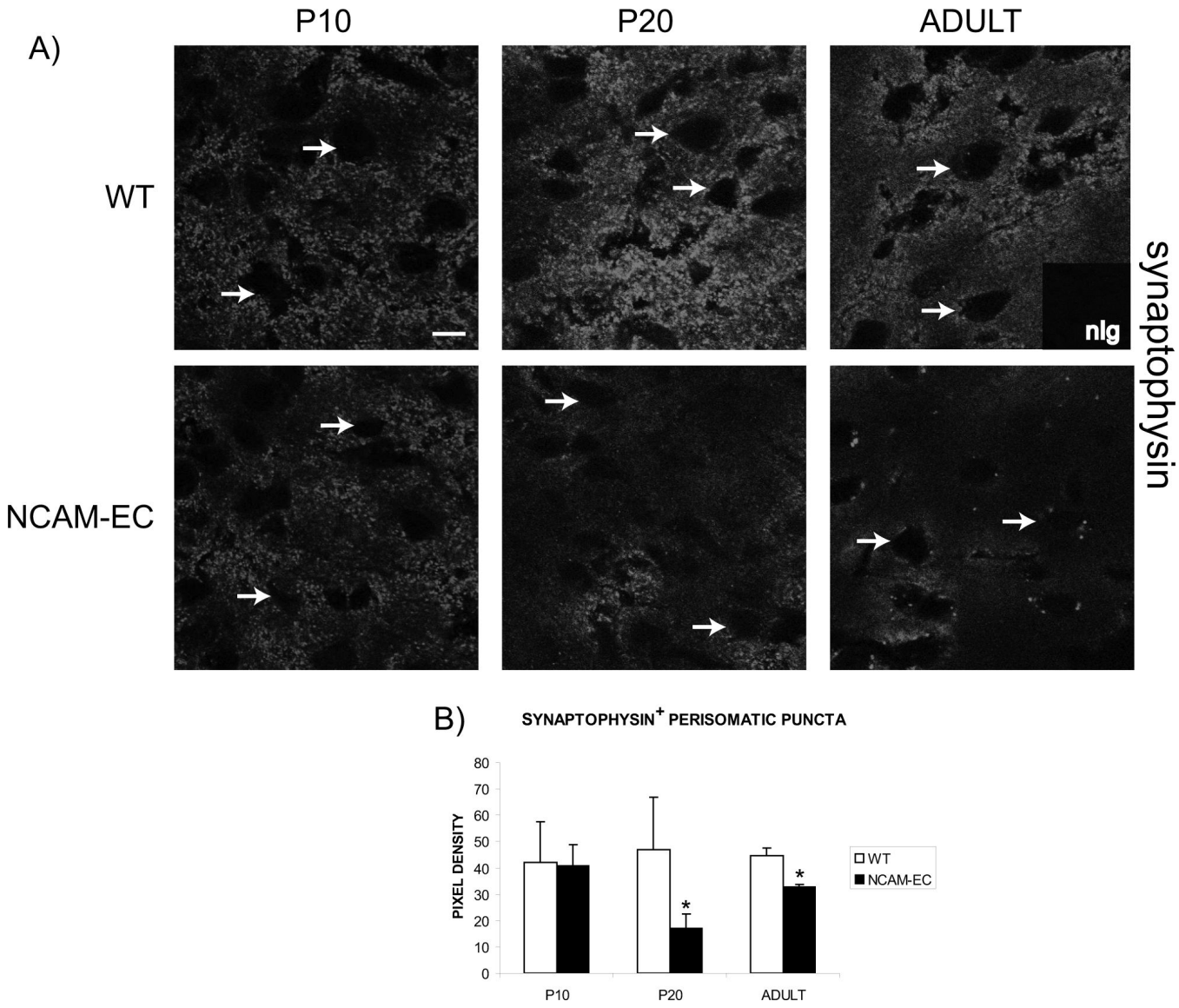


**Figure 6. Excitatory synapse development is perturbed by NCAM-EC**

A) Representative images of synaptophysin immunofluorescence from layer II/III of the PFC of WT and NCAM-EC transgenic mice at P10, P20 and adult stages. Arrows indicate the location of soma. Nonimmune Ig control is included as an inset. Scale bar = 10 μm. B) Pixel density of perisomatic synaptic puncta rings. Four images were analyzed for each animal and 3 animals per genotype per stage were analyzed. Student's t test *$p<0.06$.

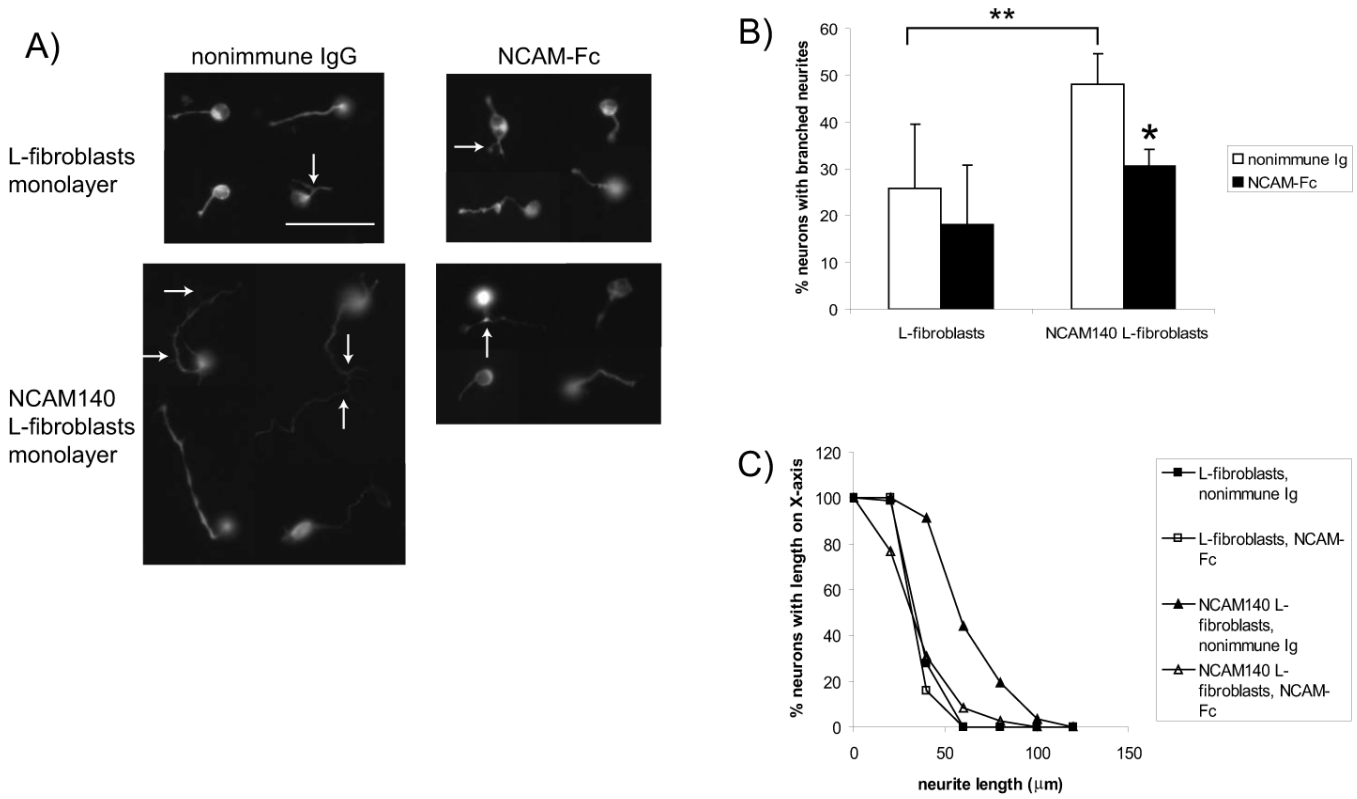


**Figure 7. Soluble NCAM extracellular domain inhibits neurite outgrowth and branching in culture**

A representative experiment is shown. Four wells for each condition were analyzed and at least 150 neurons were analyzed per condition. A) Cortical neurons were plated onto monolayers of L-fibroblasts or L-fibroblasts expressing NCAM140 and neurites allowed to extend for 72 h in the presence (black bars) or absence (nonimmune Ig, white bars) of NCAM-Fc before being visualized using TUJ1 immunofluorescence. Arrows indicate branched neurites. Scale bar = 50 μm. B) The percent of neurons with branched neurites was calculated. Student's t test *$p<0.05$, **$p<0.005$. C) The cumulative percentage of neurons of a given length was determined by subtracting the percent of neurons with length X from 100 as described previously (Beggs 1994; Hinkle 2006).

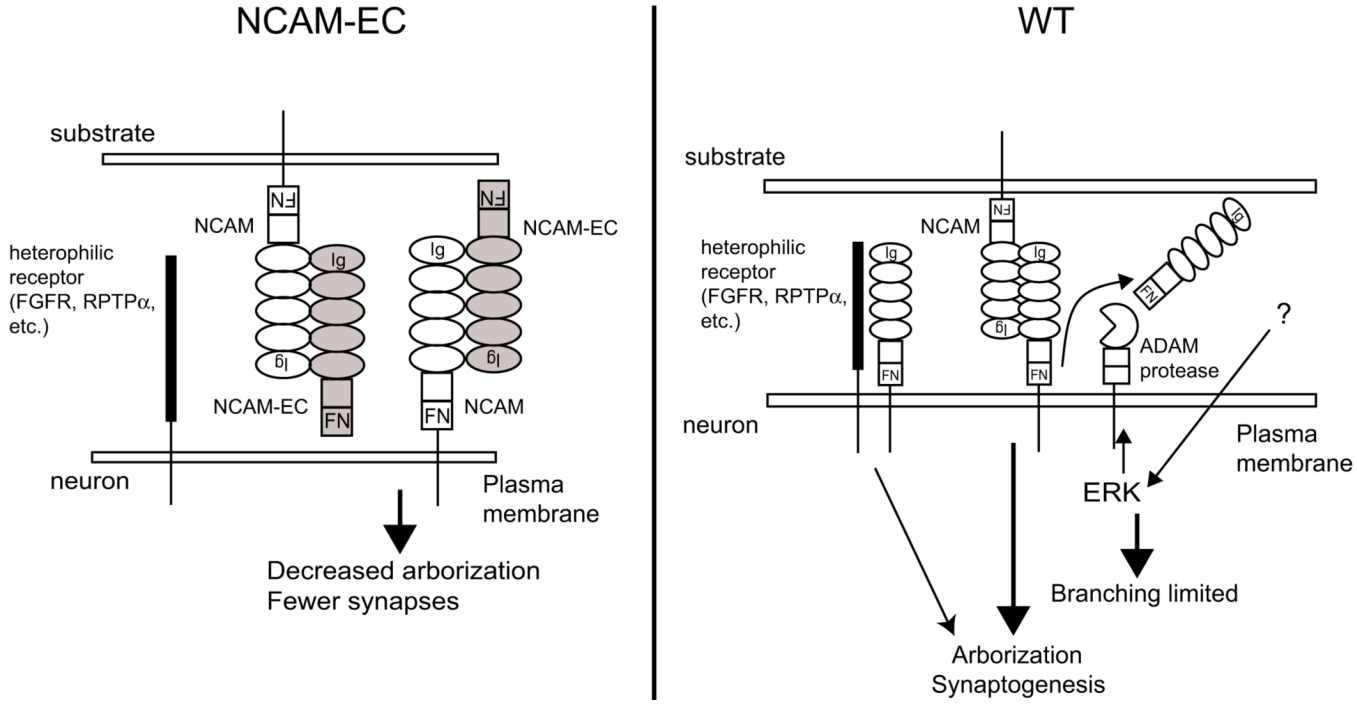


**Figure 8. Model for the mechanism of action of the shed NCAM extracellular domain in interneuronal development**

Excess soluble NCAM-EC is depicted to interact with neuronal NCAM to inhibit NCAM-NCAM homophilic binding and heterophilic interactions with receptors such as the FGF receptor (FGFR) (Meiri 1998; Kiselyov 2003; Kiselyov 2005) or receptor protein tyrosine phosphatase alpha (RPTPα, (Bodrikov 2005)), thereby decreasing interneuron arborization to result in fewer perisomatic synapses. Alternatively, in other cell types where metalloprotease-induced soluble NCAM-EC promotes neurite growth (Meiri 1998; Hubschmann 2005; Kalus 2006), transgenic NCAM-EC might bind and inhibit this activity. In normal development, ERK MAP kinase, triggered by an external stimulus, activates an ADAM family protease to cleave NCAM and release NCAM-EC. This serves to limit interneuron branching promoted by NCAM homophilic or heterophilic binding.